Image Cover Sheet

CLASSIFICATION	SYSTEM NUMBER
UNCLASSIFIED	514410

TITLE

Remote Performance Prediction for Infrared Imaging of Buried Mines

System Number:

Patron Number:

Requester:

Notes:

DSIS Use only:

Deliver to:

This page is left blank

This page is left blank

Remote Performance Prediction for Infrared Imaging of Buried Mines

Kevin Russell, John McFee and Wayne Sirovyak

Threat Detection Group, Defence Research Establishment Suffield,
Box 4000, Medicine Hat, AB, Canada, T1A 8K6

ABSTRACT

Infrared imagers are being investigated by several groups for use in landmine detection. The ability to predict detection performance is necessary to establish confidence for single sensor systems or to allow appropriate weighting of detector output for data fusion algorithms in multiple sensor systems. Preliminary studies had shown that the in-ground vertical temperature gradient was a good indicator of mine/background contrast in infrared images if temperature measurements and imager were colocated and limited data suggested that remote performance monitoring might be possible. To establish practicality of remote monitoring, temperature probes were buried at 5 sites separated by various distances between 30 m and 5.8 km, in asphalt, sand and gravel, both on and off road. Vertical temperature profiles were automatically recorded at all sites simultaneously with infrared images of buried thermal IR surrogate mines located at a gravel road site. The in-ground vertical temperature gradient was confirmed to be a practical indicator of the performance of an IR imager, for probes buried in all materials at distances up to almost 6 km from the imager. A five element probe with thermocouples uniformly placed at depths from -3 to -11 cm would be sufficient to predict detection performance.

Keywords: Infrared imaging, Mine detection, Thermal Gradient

1. INTRODUCTION

The Research and Development Branch of the Canadian Department of National Defence, in support of Canadian peacekeeping activities, has undertaken a development project for the detection of modern landmines.[1] The Improved Landmine Detection Project (ILDP) will produce a multisensor, remotely operated vehicle that has a high probability of detection of on-route anti-tank landmines coupled with a low false alarm rate. Comprising the four most suitable landmine sensors indicated in the Research and Development Branch Countermine Study,[2] the resulting system must operate in a wide range of environmental conditions. Given that the performance of these sensors is a function of changing environmental conditions, it is desirable to predicate the performance of each sensor. This is necessary to assess the individual detection capability of each sensor in advance of a mission and to also allow appropriate weighting when combining the sensor outputs.

Of the chosen sensors, the 8-12 μm wavelength passive infrared imager is by far the most dependent upon environmental conditions. The performance can degrade during the inversion period of the diurnal cycle, unfavourable air temperature, cloud cover, and other factors.[3] A preliminary study[4] showed that the in-ground vertical temperature gradient was a good indicator of mine/background contrast in infrared images. In-ground temperature probes were situated at the same site as the imaged buried mines for most of the study. For logistical reasons, it is desirable to predict performance using an in-ground temperature probe placed at a distance. A single experiment was done which showed that temperature gradient data at two sites 3.5 km apart were correlated in time, but it was difficult to generalize since time sample spacing and range were limited, a few times were noted where correlation was inexplicably poor and the two sites were on the same packed gravel road.

Other author information: (Send correspondence to K.R.)
K R.: Email. Kevin.Russell@dres.dnd.ca, Telephone: 403-544-4746; Fax: 403-544-4704;
J M.: Email. John.McFee@dres.dnd.ca, Telephone 403-544-4739, Fax. 403-544-4704
W.S.: Email: Wayne.Sirovyak@dres dnd ca; Telephone: 403-544-4735; Fax: 403-544-4704
Supported by the Research and Development Branch, Department of National Defence, Canada, under Project Numbers 2HB11 and 2HE11.

In the present study, temperature probes were buried at 5 sites separated by various distances between 30 m and 5 km, in asphalt, sand and gravel, both on and off road. Vertical temperature profiles were automatically recorded at all sites simultaneously with infrared images of buried thermal IR surrogate mines from one site. Correlations of temperature gradients between sites and with mine/background image contrast values are presented and discussed in the context of remote prediction of infrared image performance.

2. PROCEDURE

Five temperature probes* were buried in identical fashion one week prior to the experiment at different sites consisting of a gravel road, a sand road (30 m from the gravel road), an asphalt road (880 m), a graveled equipment yard (3860 m), and a graveled parking lot (5830 m). Each temperature probe had sixteen T-type thermocouples placed 2 cm apart and, when buried, the top thermocouple was exposed to ambient conditions 1 cm above the ground surface. To insure good contact between the temperature probes and the surrounding earth, sand was packed around the probe to reduce any air gaps created by the drilling process. Four data acquisition computers were used to monitor the temperature probes, with the probes at the gravel and sand roads sharing a single computer.

Two sets of IR surrogate mines, each consisting of an anti-tank (AT) simulant and two anti-personnel (AP) simulants, were buried in the gravel road. One set was buried one week prior to the experiment and the other set had been buried for over a year. An Agema Thermal Vision 1000 camera with a 62(h)x41(v) degree FOV was positioned 3 m above the ground and inclined downward from the horizontal plane by 40 degrees such that the buried surrogate mines appeared in the bottom half of the image. This geometry is similar to that used in vehicle mounted systems, such as the ILDP system.

Every 15 minutes over a period of 48 hours, data from the temperature probes and a digital 800x400x12bit IR image were collected. Care was taken to insure that the data collection was well synchronized in time between the four computers monitoring the temperature probes and the one computer controlling the IR image acquisition. Possible clock drift between the machines was monitored and was found not to be significant. The data acquisition cycle for each temperature probe involved sampling each thermocouple junction in sequence, repeating 100 times over a total period of 60 seconds, and computing an average and standard deviation.

3. ANALYSIS

For each probe location and time, the vector of temperature values versus depth obtained from the thermocouple junctions was numerically differentiated with respect to depth using a 3-point, Lagrangian interpolation. This yielded a time series of vertical temperature gradient values for each depth increment for all probe locations. The linear correlation coefficients between the time series of the temperature gradient at each thermocouple junction at the gravel road site and that of the thermocouple junctions at the other probe sites at the corresponding depth were calculated using the following method and presented in Table 1.

The linear correlation coefficient is routinely used in statistical applications as a parameter to evaluate the degree of correlation between two series of measurements. Let $\vec{x} = (x_1, x_2, ..., x_n)^T$ be a time series vector of temperature gradient values from one site and let $\vec{y} = (y_1, y_2, ..., y_n)^T$ be a time series vector of temperature gradient values from a second site. The linear correlation coefficient, r, is defined[5] as

$$r(\vec{x}, \vec{y}) = \frac{(\vec{x} - \bar{x}\vec{e})^T (\vec{y} - \bar{y}\vec{e})}{\|\vec{x} - \bar{x}\vec{e}\| \, \|\vec{y} - \bar{y}\vec{e}\|} \tag{1}$$

where the superscript, T, denotes the transpose of the vector and $\|\vec{u}\|$ denotes the norm of vector $\vec{u}$. The constant n-space vector $\vec{e}$ is defined as $\vec{e} = (1, 1, 1, ...1)^T$. $\bar{x}$, $\bar{y}$ are the arithmetic means of the elements of vectors $\vec{x}$, $\vec{y}$ respectively,

$$\bar{x} = \frac{1}{n}\vec{x}^T\vec{e} \quad , \quad \bar{y} = \frac{1}{n}\vec{y}^T\vec{e} \; . \tag{2}$$

*manufactured by Geotherm Inc., 160 Pony Dr , Unit #6, Newmarket, Ontario, Canada, L3Y 7B6, (905) 953-0698

If $\vec{x}, \vec{y}$ are linearly related with no uncertainty, i.e., $\vec{y} = a\vec{x} + b\vec{e}$, where a, b are scalars which are not functions of $\vec{x}$ or $\vec{y}$, then $|r| = 1$. In other words, the series of measurements are perfectly correlated with time. On the other hand, $r = 0$ indicates that $\vec{x}, \vec{y}$ are not linearly related and the series of measurements are completely uncorrelated with time. Although intermediate values must be interpreted in a statistical context, values of 0.9 or more generally indicate very good correlation for large sample sizes such as occur in these experiments ($N \approx 200$).

As in previous studies,[3,4] the apparent temperature contrast for each mine site in an IR image was calculated by subtracting from the pixel-averaged value of a small area at the center of the blob created by the buried mine, the pixel-averaged value of a reference area close to the mines. Plots of apparent temperature contrast versus time for all mines are presented in Figure 4.

4. RESULTS AND DISCUSSION

Figure 1 shows how the temperature at each thermocouple junction varied over the 48 hour period at the gravel road site. Standard deviations in the individual recorded temperature measurements were mostly less than 0.1 C, although occasionally in the 0.1 to 0.5 C range. Standard deviations were slightly higher for the asphalt site than for the other sites. A periodic variation with a period roughly equal to a day is seen for all depths. The amplitude of the variation decreases with depth and there is also a depth dependent phase lag. This is not surprising, since temperature variations are ideally modelled by a diffusion law. There was insufficient time in this study, however, to fit the temperature variations to a model. The first junction, located at 1 cm above the ground surface, fluctuates over a 30 C range, which is slightly greater than is typical for ambient mid-summer temperatures in South East Alberta. This increase over ambient is due in part to reflection of the incident solar radiation from the ground surface and to boundary layer effects near the surface. The other four sites have similar temperature profiles and have not been plotted here. The only deviations to the presented profile were observed at two sites where a few abrupt, large temperature excursions of relatively short duration were discovered in the data. These temperature spikes can be attributed to temperature induced offsets in the data acquisition hardware. Luckily, the shift in the data was identical for all thermocouple junctions for a given time sample, allowing correct calculation of the temperature gradient.

Inspection of table 1 reveals that temperature gradients for a given depth are well correlated from site to site, provided the measurement depth is between roughly -3 cm and -15 cm. A decrease in correlation is observed at shallower depths, presumably due to surface differences. Correlation is roughly the same for the gravel and sand sites and is slightly poorer for the asphalt road. This is likely due to the difference in surface and subsurface material between the sites. This is further confirmed by the more rapid fall off in correlation with large depths of the asphalt road, compared to the sand and gravel sites. There is no apparent decrease in correlation with distance between sites. This shows that the temperature gradient does not have to be measured locally and that probes can be installed up to 5.8 km from a site and still accurately estimate the temperature gradient at the site. It also shows that the choice of road surface in which the probe is buried is not critical.

Figure 2 and figure 3 show respectively the best nighttime and daytime IR images observed during the experiment. The three dark blobs in the left bottom of figure 2 are caused by the recently buried mine surrogates with the larger blob corresponding to the AT surrogate. Likewise the three dark blobs in the right bottom are caused by the long-buried surrogates. The same configuration of surrogates can be seen in figure 3, but the blobs are light. As discussed in previous work,[3,4] the right hand blobs of figure 3 demonstrate the "volume effect" in which the mine's IR contrast is due solely to the presence of the buried mine. The left hand blobs of figure 3 show the "surface effect" whereby the IR contrast is primarily due to the disturbed soil layer covering the mine. These effects are also seen in the nighttime image figure 2, but the "surface effect" is less pronounced.

The time variations of the apparent temperature contrast for each mine site, calculated from the IR images, are presented in figure 4. The general diurnal cyclical behaviour is readily apparent, as are "cross over" periods when contrast is very near zero and hence mines are undetectable. The large spike that appears in the left bottom AP graph and the smaller spikes that appear in the other graphs are caused by shading due to the IR camera mounting structure. Part of the shadow caused by the mounting structure can be seen in the lower left corner of figure 3. The shadow moved across the image in the day light hours partly or completely covering all the mine sites, with the exception of the far left AP site.

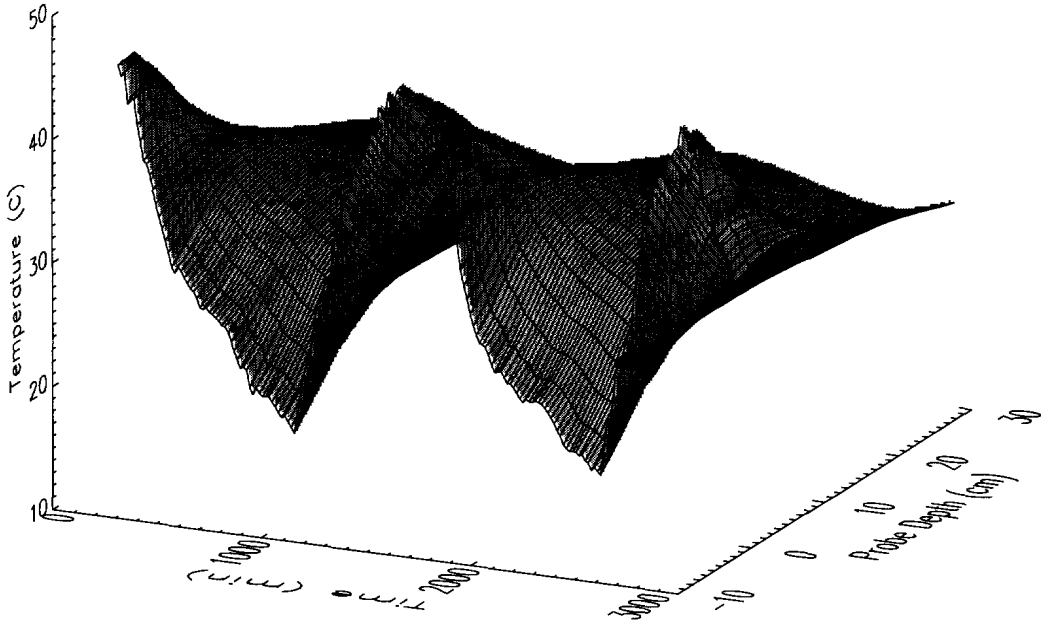

Figure 1. Temperature profile under the gravel road. Time is measured from the start of the experiment (1631 hours Mountain Daylight Savings Time, August 14, 1996).

Table 2 presents the linear correlation coefficients calculated for each probe depth under the gravel road and each mine site. Each coefficient measures the degree of correlation in time of the temperature gradient for a given depth with the apparent temperature contrast (measured from IR images) of a given mine site. Similar results were obtained for the other probe sites but are not presented here. Very high correlations are observed at almost all sites, with coefficients greater than 0.9 for a depth range between 4 and 6 cm. Maximum values are roughly independent of mine type and age of burial. The one exception is the bottom left AP mine, whose correlation is good, but significantly less than the other mines (maximum correlation coefficient $\sim$0.8 for a depth range of 4 cm). The latter is likely due to the overall lower contrast of that recently buried AP mine. This confirms that the temperature gradient is a good indicator of apparent temperature contrast for mines in IR images and hence is a good predictor of performance of an IR imager for mine detection.

For each mine, correlation coefficients first increase with increasing depth, reach a maximum and then decrease. The poor correlation near the surface is likely due to surface effects, which also caused poor temperature gradient correlations between probes. The decrease in correlation with depth likely occurs because the mines disturb heat flow at shallow depth, but have a decreasing effect on heat flow as depth increases. Table 3 shows the depth at which the highest linear correlation coefficient between the temperature gradient and the apparent temperature contrast occurs for each mine site. The values for each mine site are the mean and standard deviation derived from the maximum depth for the mine site for all probes. There is a spread in depth of maximum, with the depth for AT mines being slightly greater than for AP, presumably due to the deeper excavation required to emplace the AT mines. From

Table 1. Linear correlation coefficients calculated for each thermocouple depth under the gravel road and corresponding depths for all other probe sites. Coefficients measure the degree of correlation in time of the temperature gradient between two sites at a given depth.

Depth (cm)	Parking Lot	Asphalt Road	Equipment Yard	Sand Road
1	0.0533	0.4123	-0.4337	-0.1980
-1	0.8378	0.8765	0.8949	0.8680
-3	0.9654	0.9556	0.9582	0.9864
-5	0.9856	0.9761	0.9853	0.9940
-7	0.9905	0.9820	0.9887	0.9962
-9	0.9935	0.9884	0.9928	0.9977
-11	0.9953	0.9893	0.9917	0.9985
-13	0.9951	0.9863	0.9867	0.9990
-15	0.9957	0.9798	0.9849	0.9992
-17	0.9964	0.9619	0.9748	0.9993
-19	0.9953	0.9443	0.9686	0.9986
-21	0.9953	0.9441	0.9759	0.9966
-23	0.9952	0.9219	0.9797	0.9969
-25	0.9965	0.8822	0.9659	0.9989
-27	0.9968	0.8632	0.9587	0.9988
-29	0.9864	0.8217	0.9512	0.9825

tables 2 and 3, it can be seen that a five element probe with thermocouples uniformly placed at depths from -3 to -11 cm would be adequate to predict IR imager performance if the temperature probe were at the site of the IR imager. Recalling that the highest correlations between temperature gradient measurements at different probe sites occurred within the depth range of -3 to -15 cm, a five element thermocouple probe should then be able to adequately predict IR imager performance for mine detection if buried within 5.8 km of the IR imager site.

5. CONCLUSIONS

Experiments have shown that the in-ground vertical temperature gradient is a practical indicator of the performance of an IR imager for detection of landmines buried in roads. The gradient may be measured using a thermocouple probe buried in the ground at distances up to 5.8 km from the IR detection site. Probes buried in asphalt, gravel and sand all give similar results and the results are independent of distance between the probe and the IR imager. A five element probe with thermocouples uniformly placed at depths from -3 to -11 cm should be sufficient to predict detection performance.

Future work should look at extending the distance over which IR imager detection performance can be predicted. The experiments should be repeated for other ambient conditions, particularly cooler temperatures, and for images on other types of roads and ground surface covers. Probe burial in other ground materials should be investigated as well. Preliminary inspection of data suggested that the standard deviation of the apparent background temperature in the IR imagery may be weakly correlated with the temperature gradient near the surface. This may form an additional indicator of IR detection performance and should be further investigated.

6. ACKNOWLEDGMENTS

We wish to thank Mr. Jason Edwards for his assistance in setting up the experiment and in collecting and analysing the data.

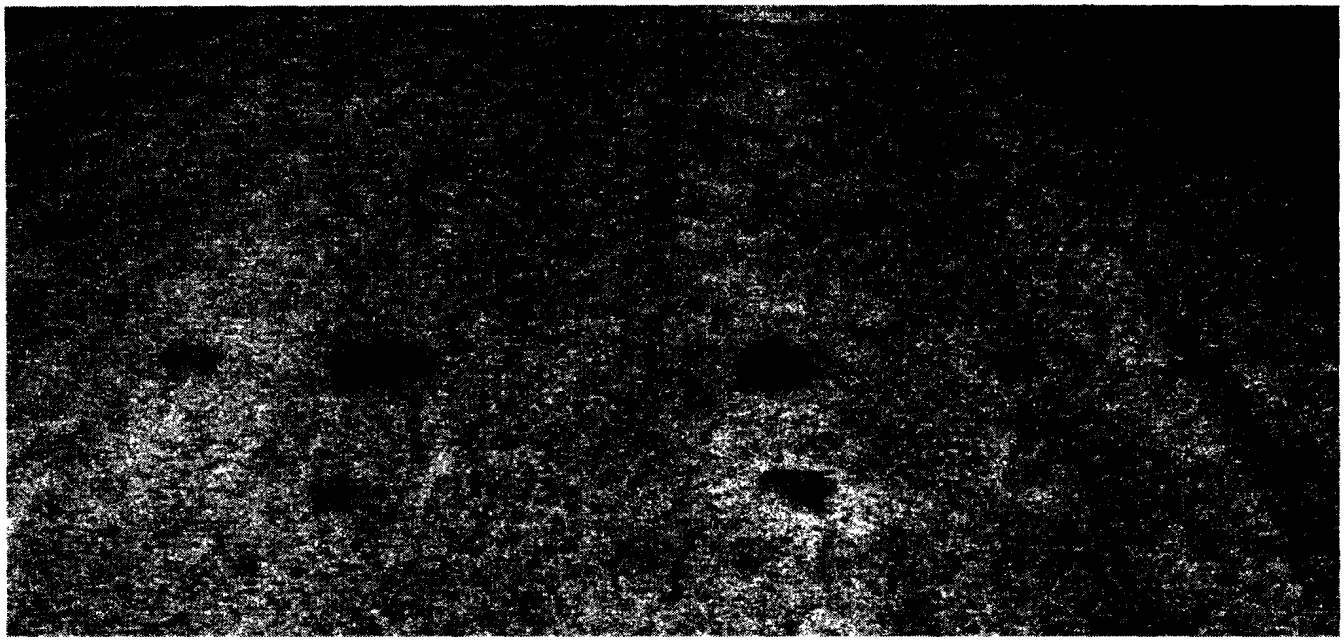

Figure 2. Nighttime IR image (0445 hours)

REFERENCES

1. J.McFee and A.Carruthers, "A multisensor mine detector for peacekeeping - Improved Landmine Detector Concept (ILDC)," in *Detection and Remediation Technologies for Mines and Mine-like Targets*, A.C.Dubey, R.L.Barnard, C.J.Lowe, and J.E.McFee, eds., *Proc. SPIE* **2765**, pp. 233–248, 1996.
2. J.E.McFee, Y.Das, A.Carruthers, S.Murray, P.Gallagher, and G.Briosi, "CRAD countermine R&D study - Final Report (U)," Report SSP 174, Defence Research Establishment Suffield, April 1994.
3. J.R.Simard, "Experimental evaluation of the apparent temperature contrast created by buried mines as seen by an IR imager (U)," Report SR 607, Defence Research Establishment Suffield, November 1994.
4. J.R.Simard, "Improved landmine detection capability (ILDC): systematic approach to the detection of buried mines using passive IR," in *Detection and Remediation Technologies for Mines and Mine-like Targets*, A.C.Dubey, R.L.Barnard, C.J.Lowe, and J.E.McFee, eds., *Proc. SPIE* **2765**, 1996.
5. J.E.McFee, S.Achal, and C.Anger, "Scatterable mine detection using a *casi*," in *Proceedings of the First International Airborne Remote Sensing Conference*, pp. I587–598, Environmental Research Institute of Michigan, (Strasbourg, France), September 1994.

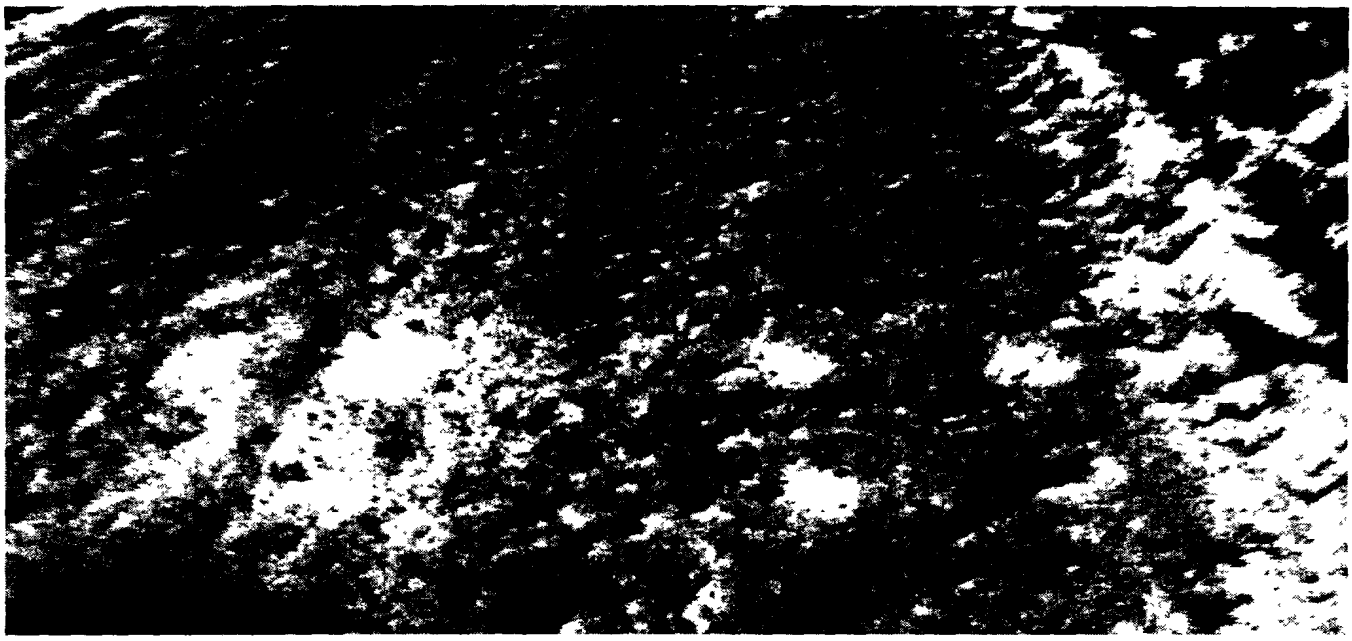

Figure 3. Daytime IR image (1415 hours)

Table 2. Linear correlation coefficients calculated for each probe depth under the gravel road and each mine site. Coefficients measure the degree of correlation in time of the temperature gradient for a given depth with the apparent temperature contrast (measured from IR images) of a given mine site.

Depth (cm)	Left AT	Far Left AP	Bottom Left AP	Right AT	Far Right AP	Bottom Right AP
1	0.7380	0.7784	0.7249	0.5762	0.8493	0.6491
-1	0.8816	0.9084	0.8103	0.7686	0.9539	0.8600
-3	0.9270	0.9407	0.8132	0.8647	0.9589	0.9395
-5	0.9509	0.9513	0.7984	0.9255	0.9370	0.9599
-7	0.9423	0.9282	0.7591	0.9497	0.8841	0.9516
-9	0.9133	0.8890	0.7162	0.9489	0.8294	0.9257
-11	0.8715	0.8368	0.6593	0.9333	0.7586	0.8834
-13	0.8085	0.7608	0.5848	0.8930	0.6622	0.8203
-15	0.7211	0.6599	0.4940	0.8278	0.5457	0.7326
-17	0.5956	0.5212	0.3710	0.7257	0.3910	0.6070
-19	0.4632	0.3781	0.2483	0.6085	0.2377	0.4722
-21	0.3766	0.2852	0.1748	0.5265	0.1437	0.3836
-23	0.2353	0.1391	0.0554	0.3962	-0.0030	0.2402
-25	0.0485	-0.0498	-0.1013	0.2155	-0.1916	0.0499
-27	-0.0695	-0.1678	-0.1933	0.0920	-0.3059	-0.0716
-29	-0.1407	-0.2376	-0.2422	0.0134	-0.3676	-0.1494

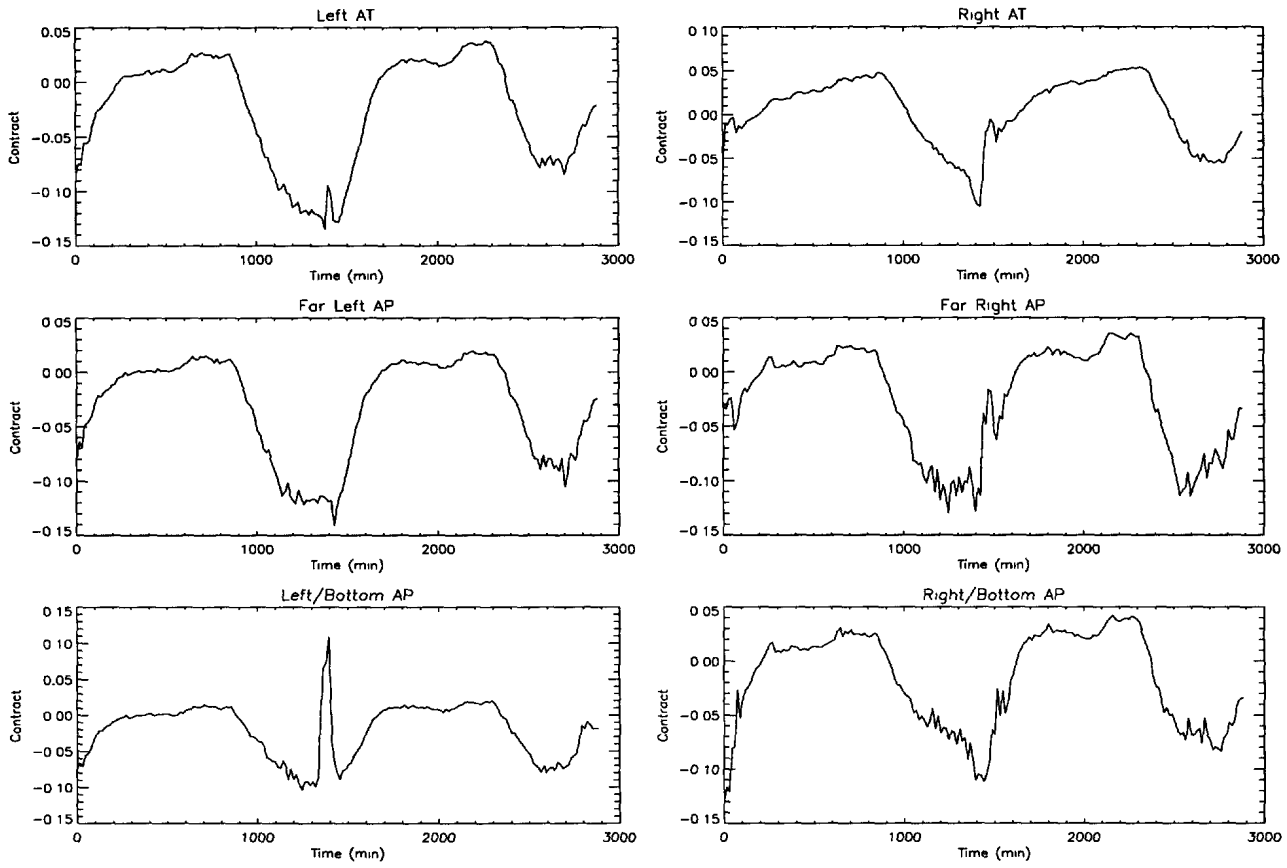

Figure 4. Time variation of the apparent temperature contrast of the six mine sites. Time is measured from the start of the experiment (1631 hours Mountain Daylight Savings Time, August 14, 1996).

Table 3. Depth at which the highest linear correlation coefficient between the temperature gradient and the apparent temperature contrast occurs for each mine site.

Left AT	Far Left AP	Bottom Left AP	Right AT	Far Right AP	Bottom Right AP
-6.2 ±1.1 cm	-5.0 ±1.4 cm	-3.8 ±1.1 cm	-9.0 ±1.4 cm	-4.2 ±1.1 cm	-5.8 ±1.1 cm